

Experimental Investigation of Aero-Hydroelastic Instability Parameters of the Deep-Water Hydrohoist Pipeline

*Yevgen Oleksiyovych Kyrychenko, Volodymyr Illich Samusya,
Volodymyr Yevgenovych Kyrychenko and Artem Valeriyevich Romanyukov*

State Higher Educational Institution National Mining University, Dnipropetrovsk, Ukraine

Abstract: The article contains the results of experimental research of unstable aeroelasticity type of wind resonance and galloping for the elements of pipeline of deep-water hydraulic handling. The experiments have been carried in aerodynamic pipe on a scale models while using the strain measure balance. The laws exposed and some qualitative results can be useful while investigating the self-excited oscillating of the constructions under the influence of wind load.

Key words: Instability • Cylinder • Fluid dynamics • Hydrohoist • offshore mining

INTRODUCTION

Each known problem solving of elastic construction dynamics under the influence of wind loads supposes there is indispensable for the calculations information about aerodynamic forces which can be obtained experimentally only. This is the main trouble of all aeroelastic problems as to obtain reliable information concerning the working aerodynamic forces needs a great number of experiments and finally it is connected with sizeable expenditures than subsequent motion equation solution [1-6]. In this connection the practical significance of similar investigations exceeds the bounds of oscillating bodies [6] behavior in a wind flow owing to technical actuality of analogous researches for liquid flowing rod construction, for example, submarine pulp feed-lines. That's why it is advisable to considerate from the scientific point of view more common problem of self-excited oscillation beginning mechanism for elastic constructions being flown by air or liquid.

While designing the construction to be interacted with the flow it is necessary to pay much attention to its element oscillation calculations to find such geometric and dynamic characteristics which can exclude possible self-excited oscillation excitation.

Each section of pipe-line is a set of pipe-lines. Intake pipe-line is the main one and it is surrounded with some auxiliary pipe-lines which have less diameter.

There were tested some set lay-out with fixed disposition pipe-lines of selected diameters one of which (set 1) is in Figure 1 and set 2 (Figure 2) to study according to geometrical parameters l and φ . For set 1: $d_1 = 0.33$; $d_2 = 0.22$, $d_3 = 0.1$, $d_4 = 0.06$, $r_1 = 0.79$, $r_2 = 0.74$, $r_3 = 0.66$, $r_4 = 0.62$ For set 2: $d_1 = 0.33$; $d_2 = 0.19$, $d_3 = d_4$, l and φ have being ranged ($\varphi = \varphi_0$ means the pipe-lines d_2, d_3 and d_4 touch on each other). Here and below all linear dimensions are referenced to the diameter of central pipeline d . In the experimental aerodynamic model d diameter was 100 millimeters.

The study of hydrodynamic instability of vortex excitation type. Vortex excitation as it is known [7] originates owing to periodical eddy separation from smooth surface of stream-lined extent elastic body. Periodical eddy separation form so called Karman vortex trail in the wake of the body. The frequency of f_0 vortex separation is determined by the Strouhal number: $Sh = \frac{f_0 d}{V}$.

For each section made fast in the flow the Strouhal number has quite definite value (which will depend upon the angle of incidence too if profile is asymmetrical one). For single cylinder $Sh \approx 0.2$. Owing to periodical vortex separation (either from one side of cylinder or from another one) pressure distribution along its surface gains periodical component therefore cross force Y_D with f_0 frequency arises and resistance X_D force gains periodical addition which frequency is $2f_0$:

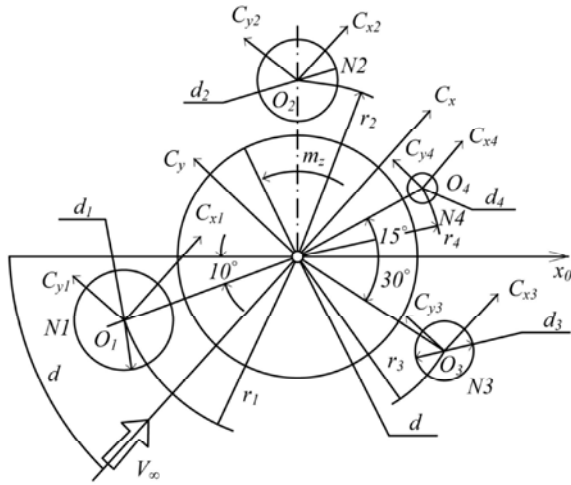


Fig. 1: Set 1 Scheme.

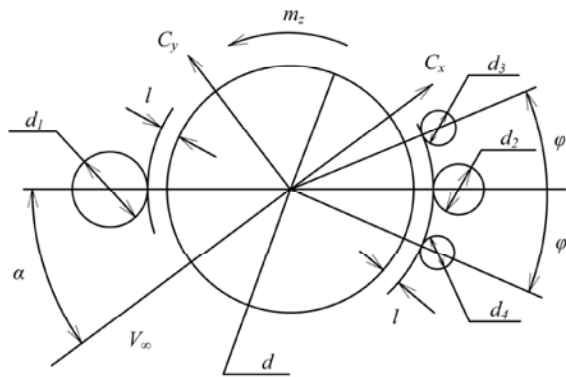


Fig. 2: Set 2 Scheme to study l and φ parameters.

$$Y_D = Y_{max} \sin(2\pi f_0 t) \quad (1)$$

$$X = X_{av} + X_D = X_{av} + X_{max} \sin(4\pi f_0 t)$$

where X_{av} – average (static) value of resistance force; Y_{max} and X_{max} – amplitude values of cross and resistance forces periodical components.

If we use aerohydrodynamic indices, according to (1) they will be:

$$C_y = C_{ya} \sin(2\pi f_0 t) \quad (2)$$

$$C_x = C_{x0} + C_{xa} \sin(4\pi f_0 t)$$

where C_{x0} – average value of resistance force coefficient; C_{ya} and C_{xa} – amplitude values of correspondent coefficients (each coefficient is related to $\rho V^2/2$ and d).

C_x values for set 2 are in Figure 3. As there is torque which m_z coefficient is in Figure 4, the sections of the pipe-line torsionally vibrate comparatively to longitudinal axis.

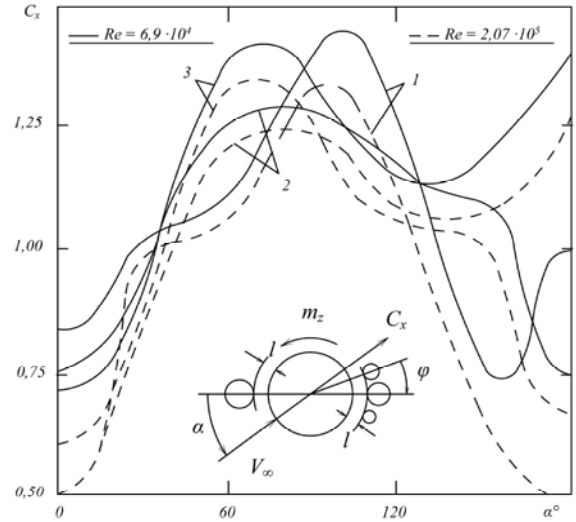


Fig. 3: Resistance force coefficient for the set 2: 1 – $\bar{l} = 0.05$; $\varphi = \varphi_0$; 2 – $\bar{l} = 0.05$; $\varphi = 30^\circ$; 3 – $\bar{l} = 0.05$; $\varphi = 45^\circ$

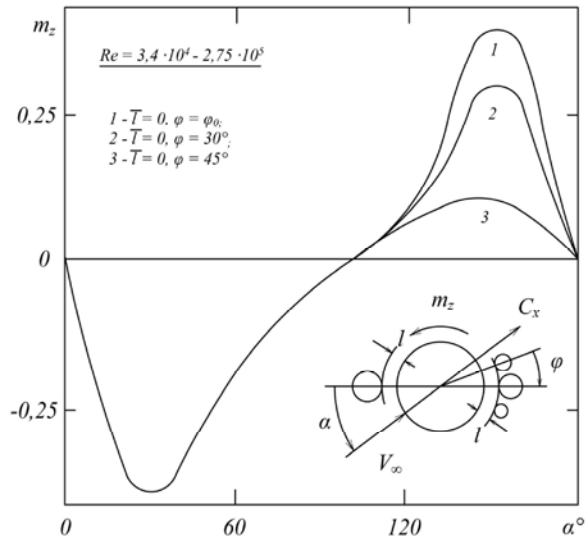


Fig. 4: Moment coefficient for the set 2.

The study of hydrodynamic instability of galloping type. The loss of hydrodynamic stability of galloping type is the beginning of extent body oscillations in diametrical direction to the flow without twist or with a small one but galloping takes place if section of the body in a definite range of angle of attack has negative gradient of hydrodynamic lift $\partial C_y / \partial \alpha < 0$ (force diametrical to flow) which is rather large as for absolute value.

The trend of self-excited oscillation regime of type of galloping beginning can be evaluated according to Den-Hartog number [8], that is section losses its stability under given angle of attack, if

$$C_y^\alpha + C_x < 0 \tag{3}$$

where C_y^α – gradient of cross force coefficient.

Figure 5 shows obtained experimental dependences of cross force coefficient of set upon angle of attack for arrangement 1 and Figure 6 – for three arrangement variants 2. As it is from the chart there are three ranges of angles of attack where derivative $\partial C_y / \partial \alpha$ is negative though condition (3) isn't satisfied in every range. For arrangement 1 (Figure 5, curve 3) derivative $\partial C_y / \partial \alpha$ value in A ($\alpha_0 = 80^\circ$) and B ($\alpha_0 = 330^\circ$) points is $\partial C_y / \partial \alpha \approx -(5-6)$ and as C_x value for this arrangement when α and Re are any (in the range to be explored) is $C_x \approx 0.75 - 1.4$, Den-Hartog number (3) is performed in A and B points and their neighborhoods $\pm 20^\circ$. On the curve 1 at the C point (Figure 3) $\partial C_y / \partial \alpha = -1.2$ and experimental value $C_x = 1.34$ a, so (3) criterion is not performed.

For 2 arrangement (Figure 6) Den-Hartog number is performed, e.g. for curve 3 in the neighborhood of A ($\alpha_0 = 60^\circ$) and B ($\alpha_0 = 300^\circ$) points. In these points $\partial C_y / \partial \alpha \approx -3.5$. Neighborhoods where (3) criterion is performed are $\pm 15^\circ$ approximately. In c point (curve 3) $\partial C_y / \partial \alpha \approx -1.3$, so if $C_x = 1.4$ (3) criterion is not performed.

Dynamic tests of aerohydroelastic self-excited oscillations of pipe-line elements. To define qualitative and some quantitative characteristics of self-excited oscillations of pipe-line there were performed direct dynamic tests of pipe-line models in air tube. Tests procedure and measuring instruments are described in detail in [9] and [10]. The tests took place with the help of specially developed multicomponent strain measurement scales which main units were mechanical resonant circuits. Their elastic and dissipative properties may be varied during the trial.

The tests have been performed on models of pipe-lines sets for different variants of arrangements. Each pipe-line itself and the whole set were separate mechanical contours where δ decrement, m mass and ω own frequency may be changed. Abovementioned strain measurement scales permitted theoretically to find the conditions of beginning and disclose the range of various types of aeroelastic instability existence according to their main signs.

Two arrangement sets shown in Figures 1 and 2 had been used for arrangement 1 gave ability to test aeroelastic self-excited oscillations of the pipe-line on the whole and every its separate pipe-line; model for arrangement 2 – the whole pipe-line only. The range of Reynolds number was $Re = 3 \cdot 10^4 - 2 \cdot 10^5$.

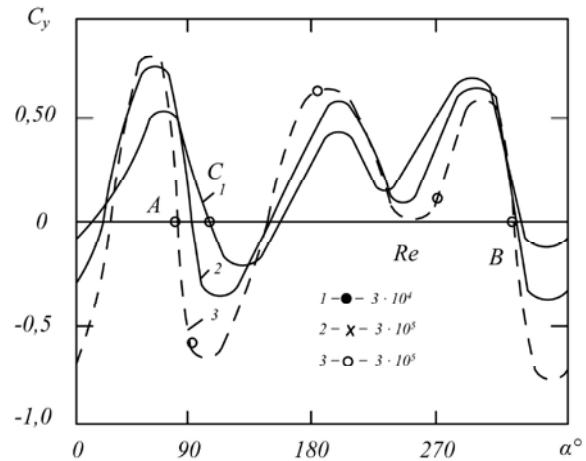


Fig. 5: The coefficient of set cross force on the whole for 1 arrangement.

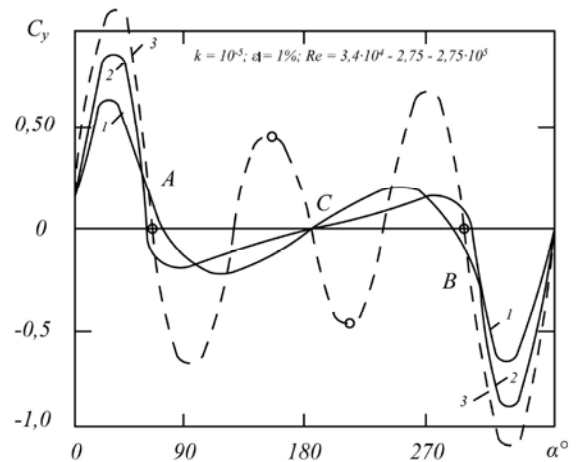


Fig. 6: The coefficient of cross force for nr.2 arrangement: 1 – $\bar{l} = 0.05$; $\varphi = \varphi_0$; 2 – $\bar{l} = 0.05$; $\varphi = 30^\circ$; 3 – $\bar{l} = 0.05$; $\varphi = 45^\circ$

The results of arrangement nr.1 model tests showed the model on the whole made flexural and torsional vibrations and some auxiliary pipe-lines – longitudinal and lateral flexural vibrations. The charts to show amplitudes of those oscillations according to Re and angle of attack are in Figures 7 and 8 (amplitudes a_{xt} longitudinal and a_{yt} lateral vibrations of each auxiliary cylinder are referred to d – diameter of central cylinder). Reynolds number for each pipe-line has been calculated in accordance with its own diameter.

As it is seen from Figure 7 the loss of aeroelastic stability for the model on the whole took place when $Re = 5 \cdot 10^4$, but for auxiliary pipe-lines in the set it happened much earlier. Figure 8 shows amplitudes of oscillations of pipe-line model as the whole. We can see

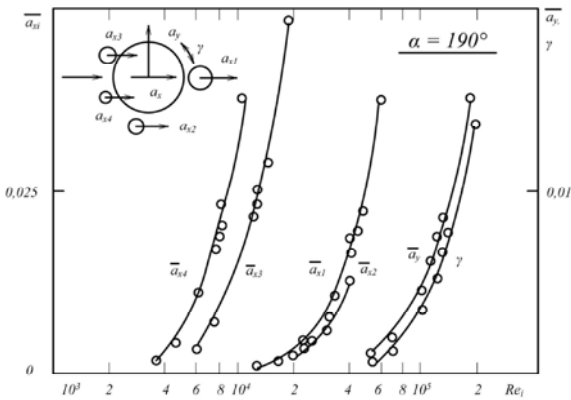


Fig. 7: The changes of kinematic parameters of flexural and torsional movement for the whole set and auxiliary pipe-lines 1 arrangement according to Reynolds number.

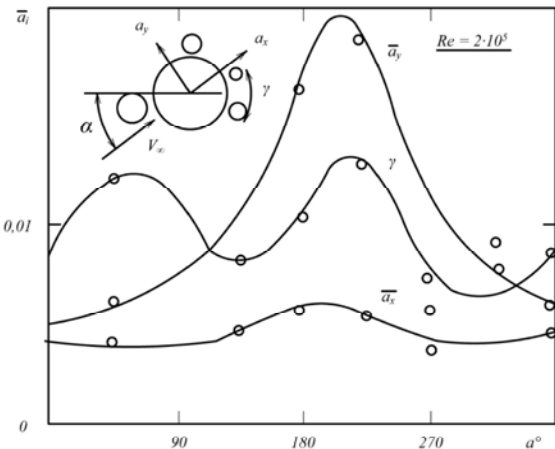


Fig. 8: The changes of longitudinal and torsional vibrations of the whole set according to angle of attack (1 arrangement).

the amplitude of longitudinal vibrations is rather less than lateral ones. The changes in flexural vibrations (that is their continuous growth from $Re = 5.10^4$ to $Re = 2.10^5$) means galloping type of self-excited oscillations in examined speed range.

As for arrangement 2, the results discovered two types of aerohydrodynamic instability losses (Figure 9): vortex excitation (*A* region) and galloping (*B* region) (the given speed is $V_{pr} = V/\omega, d$). These three cases are in accordance with following parameters: a) $\bar{l} = 0.5$; $\varphi = 30^\circ$, *A* is a region of vortex excitation ($\alpha - 0^\circ - 180^\circ$), *B* is a region of galloping ($\alpha - 0^\circ - 180^\circ$); b) $\bar{l} = 0.5$; $\varphi = \varphi_0$, *A* is a region of vortex excitation ($\alpha - 180^\circ \pm 20^\circ$), *B* is a region of galloping; c) $\bar{l} = 0$; $\varphi = \varphi_0$, *A* is a region of vortex

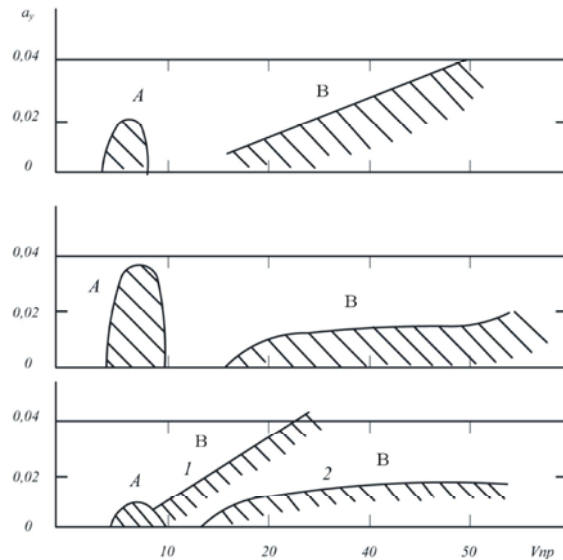


Fig. 9: Amplitude dependence of lateral oscillations of the set of speed given.

excitation ($\alpha - 0^\circ \pm 10^\circ$), *B* is a region of galloping ($1 - \alpha \approx 0^\circ$, $2 - \alpha = 20^\circ - 180^\circ$). In the region of vortex excitation the amplitude a_{yi} of lateral oscillations firstly increases when speed is picked up and then dies down; in the region of galloping the amplitude of oscillations increases as a rule with speed growth. Given results have been obtained for stiff plates, that's why amplitudes of oscillations turned out to be insignificant.

The region of self-excited oscillations of *A* vortex excitement with a given speed is $V_{pr} = 5 - 10$, or according to Strouhal number $Sh = 0.2 - 0.1$. The loss of stability of galloping type was when $V_{pr} = 14.5$. If galloping takes place both lateral and longitudinal oscillations occur with their own bending frequencies.

Instability of type of galloping was revealed in all tested ways of surrounding pipe-lines location. The most stable position as for galloping in the whole tested range of V_{pr} values and all angles of attack turned out to be the arrangement of the set when $l = 0$ (that is auxiliary pipe-lines are snug against central one).

CONCLUSIONS

The results of tests concerning the aerohydrodynamic properties of pipe-line elements showed the pipe-line cross-section which consists of pipe-line set with different diameters has inclination to display aerohydroelastic instability of type of vortex excitement and galloping. That's why any specific design needs preliminary careful aerohydroelastic tests.

Maximal possible safety of the pipe-line against hydroelastic instability beginning in the range of parameter change can be obtained by limiting the working speed of unit transportation lower than minimal stalling speed of vortex excitement beginning.

REFERENCES

1. Zhi Xing, Y. and L. Ying Zhong, 2000. Hydroelastic Calculations of Viscous Flow Around a Cylinder-Spring System. Proceedings of the Tenth (2000) International Offshore and Polar Engineering Conference, pp: 94-103.
2. Brocklehurst, P., A. Korobkin and E.I. Părău, 2011. Hydroelastic wave diffraction by a vertical cylinder. *Philos Trans A Math Phys Eng Sci.* 2011 Jul 28; 369(1947):2832-51. doi: 10.1098/rsta.2011.0110. PubMed PMID: 21690136.
3. Alekseyuk, A.I., V.P. Shkadova and V. Ya. Shkadov, 2012. Hydrodynamic instability of separated viscous flow around a circular cylinder. *Moscow University Mechanics Bulletin*, 65(5):114-119.
4. Giannetti, F. and P. Luchini, 2007. Structural receptivity of the first instability of the cylinder wake. *JFM*, 581, 167.
5. Theofilis, V., 2003. Advances in global linear instability of nonparallel and threedimensional flows. *Prog. Aero. Sciences*, 39(4): 249.
6. Arslan, T., S. Malavasi, B. Pettersen and H.I. Andersson, 2013. Turbulent Flow Around a Semi-Submerged Rectangular Cylinder. *Journal of Offshore Mechanics and Arctic Engineering*, 4: 18-28.
7. Kazakevich, M. and I. Grafski, 1984. Subharmonic entrainment of aeroelastic vibrations of circular cylinder. *Reports of AS of UkrSSR. A Series*, pp: 4.
8. Den-Hartog, G.P., 1960. *Mechanical vibrations*. Moscow: Fizmatgiz.
9. Grafski, I. and M. Kazakevich, 1983. *The aerodynamics of badly-flown bodies*. Hand book. Dnepropetrovsk: DSU.
10. Goman, O., I. Grafski and E. Kyrychenko, 1998. *Aerodynamic characteristics of immersed construction of the system for submarine extraction*. Dnepropetrovsk: NMU of Ukraine: Transaction 2.